

Dynamics of electron-electron entanglement in pulsed sinusoidal potentials

Fabrizio Buscemi,^{1,2,*} Paolo Bordone,^{3,2} and Andrea Bertoni²

¹*ARCES, Alma Mater Studiorum, University of Bologna,*

Via Toffano 2/2, 40125 Bologna, Italy

²*S3 Research Center, CNR-INFM, Via Campi 213/A, I-Modena 41100, Italy*

³*Dipartimento di Fisica, Università di Modena e Reggio Emilia, 41100, Modena, Italy*

(Dated: March 3, 2019)

We study by means of time-dependent numerical simulations the behavior of the entanglement stemming from the Coulomb scattering between two electrons subjected to a pulse of sinusoidal potential or trapped in the potential generated by surface acoustic waves. In the first case, we show how the entanglement formation depends upon the physical parameters describing the pulse switching on and off. In the second case, we find that the quantum correlation between the particles turns out to be negligible, thus validating a single-particle approach to the dynamics of such systems.

PACS numbers: 03.67.Bg, 73.63.Nm, 78.20.Bh

I. INTRODUCTION

Quantum entanglement between two charge carriers can be created when they interact through the Coulomb potential. Indeed, after a scattering the two-particle system is in general described by a two-particle state that is not separable in two single-particle pure states. This entanglement building up is an intrinsically dynamical process and its analysis is not only useful to understand the nature of the scattering process itself, but it can also contribute significantly to design quantum information processing devices. In fact, on one hand, controlled entanglement has been recognized as the fundamental resource for quantum computation and communication¹, on the other hand entanglement with the environment (i.e. decoherence) represents the main threat to the proper functioning of a feasible quantum computer². For those reasons, the study of the entanglement dynamics in scattering events

in solid-state systems has become more and more relevant in recent years^{3,4,5,6} and different proposals to produce entangled states between charged carriers, have been presented^{9,10,11}.

In this work, we analyze the time evolution of entanglement during the scattering of two electrons, in presence of a periodic potential, as the one generated by a surface acoustic wave (SAW) in a semiconductor quantum wire. However, our model and results are representative of a broader variety of situations in which the two interacting carriers are constrained in a quasi-1D domain and a sinusoidal-like potential is present.

Such kind of systems are of interest in different areas of physics, such as condensed matter¹², quantum optics¹³ and astrophysics¹⁴. In particular a great attention has been devoted to the scattering of an electron beam by a standing wave of light (the so-called Kaptiza-Dirac effect)¹⁵, stemming from the possibility of using such a system to investigate the wave nature of electrons. The latter model of matter-field interaction also raises conceptual and theoretical issues about the momentum exchange between electrons and electromagnetic radiation^{16,17,18,19}, which can be generalized to fields other than quantum optics.

As a prototype system, we consider a semiconductor quantum wire, eventually in the presence of SAWs^{20,21,22,23,24,25}. The SAWs are lattice vibrations that propagate through a semiconductor structure as longitudinal waves and can be modelled as a sinusoidal travelling electrical potential which traps the carriers in its moving minima. A number of devices exploiting SAW-electron interaction have been designed, realized and also proposed as basic building blocks for quantum computing applications, where the use of SAW has been shown to constitute a highly controllable mean to inject and drive electrons along quantum wires²¹. In fact, although the SAW technology was originally introduced in the context of metrological application for defining a new standard of electric current, it has been recognized as an important resource to improve the functionality of semiconductor quantum logic gates²¹.

The focus of the present work is on the creation of quantum entanglement between two interacting electrons, in the presence of a further external periodic potential. Specifically, we simulate numerically a two-particle scattering in a semiconductor quantum wire and determine how the tailoring of a standing pulse of sinusoidal potential is able to affect electron-electron correlation. To this aim we consider two different physical conditions: two electrons propagating in opposite directions along a 1D channel, or two electrons localized in two different minima of the periodic potential. In both cases, the two particles, are ex-

plicitely considered as indistinguishable and have the same spin. Here we intend to move a step forward in the investigation of the entanglement formation in electron-electron scattering processes, recently addressed by many works^{3,4,5,26}. We analyze how the momentum exchange between the particles affects the entanglement arising in the binary collision, and how the inclusion of an electric potential oscillating in space, e.g. a SAW pulse, modifies the entanglement dynamics. To this aim we tackle the problem by solving numerically the time-dependent two-particle Schrödinger equation and by computing, at each time step, the bipartite entanglement. Such an approach allows us to investigate also the case of a non-adiabatic switching on/off of the potential, that would make analytical techniques not applicable.

We also address another important aspect related to electron transport assisted by SAW. In fact, such a system is commonly investigated in the single-particle approximation, thus neglecting the quantum correlations. Here we want to verify whether this can be really considered a good approximation. Moreover we analyze the role played by the sinusoidal potential induced by the SAW in preventing the spreading of the wavefunction and in reducing undesired reflection effects.

The paper is organized as follows. In Sec. II, to better introduce our model system, we study the dynamics of a single free electron that is subjected to a sinusoidal potential only for a small time interval. We will refer to this case as “pulsed potential”. In Sec. III we evaluate first the entanglement generated in a collision between two electron subjected to a pulsed potential, then between two electrons localized in a steady sinusoidal potential, finally between two electron in the latter condition, when the external potential is removed for a short time interval. We comment on the results and draw final remarks in Sec. IV.

II. SINGLE-PARTICLE SYSTEM

In this section we study the dynamics of a free electron propagating in a quasi 1D system and subjected to a single pulsed sinusoidal potential. Our aim is to investigate the role played by the sine-like time-dependent potential in the time evolution of a simple single-particle wave function. The results will be of help in understanding the two-particle dynamics of the following section.

The single electron is described at the initial time $t_0 = 0$ by a minimum uncertainty

wave-packet, with the following wave function

$$\psi(x, 0) = \frac{1}{(\sqrt{2\pi}\sigma)^{1/2}} \exp\left(-\frac{(x-x_0)^2}{4\sigma^2} + \frac{i}{\hbar} p_{in} \cdot x\right) \quad (1)$$

where σ is the mean dispersion in position and p_{in} the initial momentum.

The electron feels a pulsed sine-like potential, and the Hamiltonian of the system takes the form

$$H_{on-off}(x) = -\frac{\hbar^2}{2m} \frac{\partial^2}{\partial x^2} + \Theta(t-t_{on})\Theta(t_{off}-t)A \sin(k_0 x) \quad (2)$$

where Θ is the Heaviside function, with t_{on} and t_{off} the times of turning on and off of the potential, respectively. In our numerical calculations k_0 is taken equal to the thermal electron wavevector $k_0 = \sqrt{2mk_B T}/\hbar$, for an electron in Si, where $T = 300$ K, m is the electron effective mass in Si and k_B is the Boltzmann constant. A is the amplitude of the oscillation, here fixed at 6.11 meV. The latter value corresponds to the coupling constant for the electron-optical phonon in Si²⁷.

We note that the time-dependent Hamiltonian of Eq. (2) has the same form of the one used to describe the scattering of an electron by a standing light wave. Such an interaction has been widely studied both from the theoretical and the experimental points of view^{16,17,18,19}, beginning with the the original work by Kaptiza and Dirac¹⁵. In the literature, the standing light electromagnetic potential is taken as a superposition of two counterpropagating travelling waves of identical frequency and the characteristic times of the scattering process are assumed to be much longer than the period of the wave. As a consequence, the approximation of time-average Hamiltonian can be used, this leading to the so-called ponderomotive potential oscillating in space^{16,19}.

Some peculiar aspects of the interaction between the electron and the sinusoidal wave can be understood by analyzing the dynamics of the single-particle wavefunction in the momentum representation $\phi(k, t)$, the latter being the Fourier transform of the real-space wave function $\psi(x, t)$, with $k = p/\hbar$. At the initial time, $\phi(k, 0)$ is given by a Gaussian wavepacket with a mean dispersion $1/\sigma$ centered around $k_{in} = p_{in}/\hbar$. Let us now introduce the wavefunction $\varphi(k, t)$ in the interaction picture

$$\phi(k, t) = \exp\left(-i \frac{\hbar k^2}{2m} t\right) \varphi(k, t). \quad (3)$$

Its time evolution can be evaluated by inserting Eq. (3) into the Schrödinger equation of the system, whose Hamiltonian is given in Eq. (2) for $t_{on} \leq t \leq t_{off}$. Straightforward

calculations lead to the following recurrence relation^{18,19}:

$$\begin{aligned} \frac{\partial}{\partial t}\varphi(k, t) = & -\frac{A}{2\hbar} \exp\left[i\left(\frac{\hbar k k_0}{m} - \frac{\hbar k_0^2}{2m}\right)t\right] \varphi(k - k_0, t) \\ & + \frac{A}{2\hbar} \exp\left[-i\left(\frac{\hbar k k_0}{m} + \frac{\hbar k_0^2}{2m}\right)t\right] \varphi(k + k_0, t). \end{aligned} \quad (4)$$

This represents the dynamical equation for $\varphi(k, t)$ due to the interaction between the particle and the sinusoidal potential. The two terms appearing in the rhs of the Eq. (4) have a clear physical meaning: the interaction with a potential oscillating in space allows the particle to change its momentum by an integer number of $\pm\hbar k_0$. This consideration will turn out to be fundamental to explain our results.

Under some specific conditions, approximate analytical solutions of Eq. (4) can be obtained^{17,18,19}. However, for the sake of generality, we face the problem numerically by solving the time-dependent Schrödinger equation for the electron real-space wavefunction by means of a Crank-Nicholson finite difference scheme. In Fig. 1 we report the square modulus of the wavefunction $\psi(x, t)$ given in Eq. (1) at three different time steps and for two different pulse lengths $\Delta\tau = t_{off} - t_{on}$, namely 0.1 ps and 0.2 ps. In both cases the sine potential is turned on at $t_{on} = 1$ ps and during the pulse interval the sinusoidal potential is included in the calculation of the time evolution of the system. From panel (b) we observe that shortly after t_{off} the wavepacket is not described by a smooth function anymore, but exhibits rapid oscillations that disappear at longer times. At sufficiently long times the wavefunction is split in three peaks, as can be seen from panel (c). In order to understand this behavior we need to analyze the dynamics of the momentum wave function $\phi(k, t)$, whose square modulus, after the pulse of sinusoidal potential, shows three peaks (see the inset of panel (c) of Fig. 1): one is still centered in k_{in} , while the other two are centered in $k_{in} + k_0$ and $k_{in} - k_0$. This suggests us that, for a duration of the sinusoidal pulses of 0.1 ps and of 0.2 ps, the particle is scattered by the potential and its momentum can be possibly increased or decreased by $\hbar k_0$, in perfect agreement with the prediction of Eq. (4). In this spirit we can assume that, for the case of a series of periodic pulses of the sine-like interaction, it should be expected a quantum chaotic behavior, characterized by the so-called *dynamical localization* effect, that is the non diffusive but exponentially localized momentum distribution^{29,30}. It is worth noting that the momentum gain or loss in our model depends strictly upon the duration of the pulse $\Delta\tau$. Specifically, the $\Delta\tau$ used in this work can be considered sufficient to induce a variation of $\hbar k_0$ in the electron momentum, while the

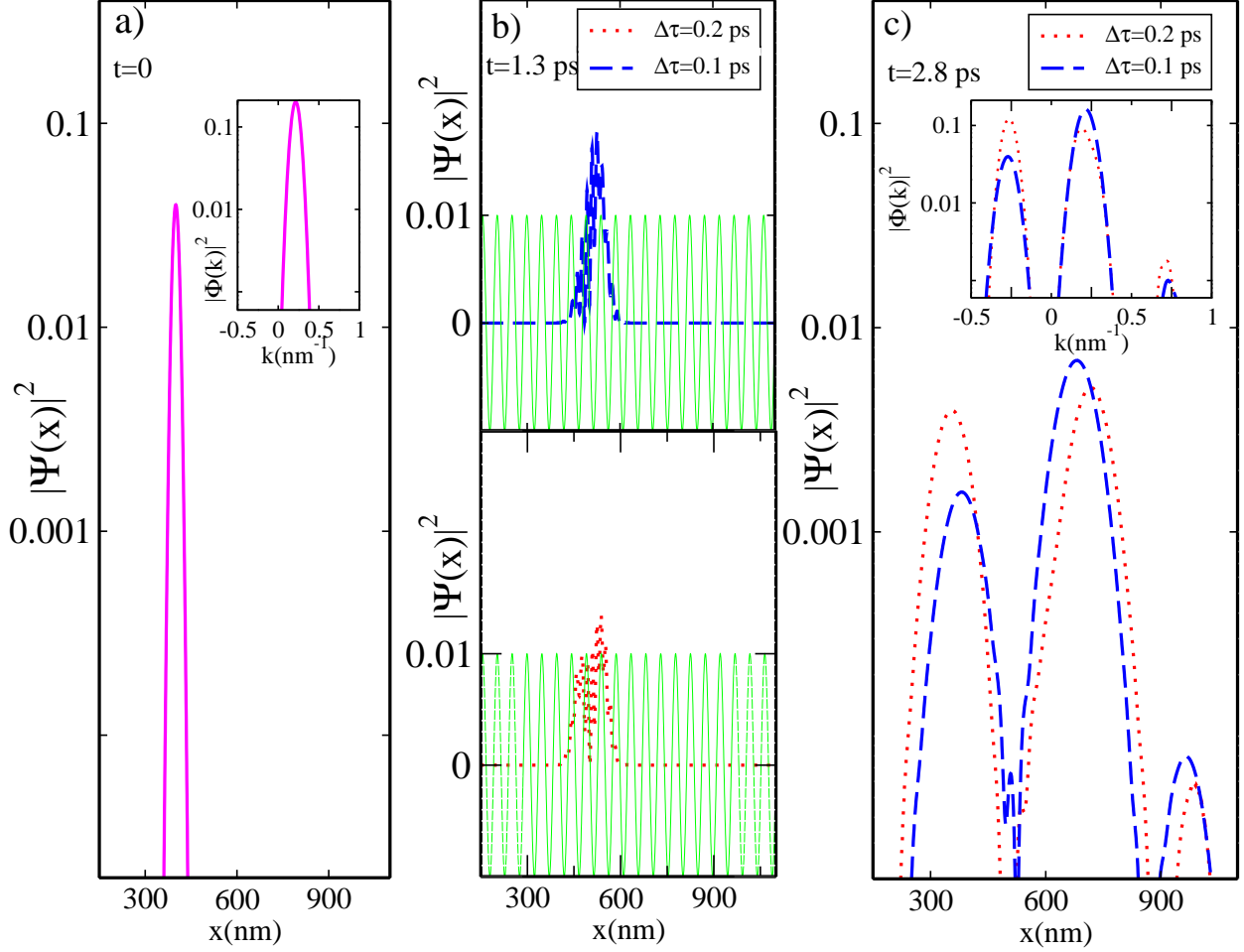


FIG. 1: (a) Square modulus of the single-electron wave function $\psi(x)$ at the initial time, with $\sigma=10$ nm and $k_{in} = 0.205$ nm $^{-1}$ corresponding to an initial kinetic energy of 5 meV. The inset shows the square modulus of its Fourier transform $\phi(k, 0)$. (b) Top panel: square modulus of the electron wavefunction $\psi(x)$ (dashed line) at $t = 1.3$ ps for a pulse duration $\Delta\tau = 0.1$ ps. (The external potential is sketched by the thin solid line). Bottom panel: same as top for $\Delta\tau = 0.2$ ps. In both cases $t_{on} = 1$ ps. (c) Comparison of the square modulus of the two electrons wavefunctions at $t = 2.8$ ps, i.e. after the pulse, for $\Delta\tau = 0.1$ (dashed line) and $\Delta\tau = 0.2$ (dotted line). The inset displays their Fourier transforms.

transfer of larger multiples of $\hbar k_0$ has a very small probability, as revealed by the negligible amplitude of the corresponding peaks in the momentum representation (not shown).

Thus, for pulses duration of 0.1 ps and of 0.2 ps, the splitting of the wavefunction into three peaks after t_{off} , has an immediate physical interpretation. The central peak gives the free evolution of the electron with momentum p_{in} while the other two describe the single-

particle free dynamics with momentum $p_{in} + \hbar k_0$, the “accelerated component” and $p_{in} - \hbar k_0$, the “reflected component”. However, we find remarkable differences in the splitting of the single-particle wavepacket when $\Delta\tau$ changes from 0.1 ps to 0.2 ps. In fact, for $\Delta\tau = 0.1$ the central peak is higher than the one of the “reflected component”, while for $\Delta\tau = 0.2$ they are very similar.

III. ELECTRON-ELECTRON ENTANGLEMENT

We now focus on the entanglement created in a two-electron scattering. The two particles interact via the Coulomb repulsion and are subject to a sinusoidal pulse, as described in the previous section. Since the entanglement formation in 1D- and 2D-scattering events between two unbound and/or trapped particles has been recently investigated^{3,4,26}, it appears of interest to study the building up of quantum correlations in such systems when a time-dependent external potential is introduced. In particular we have examined three different physical situations: an pulsed potential, a stationary potential, and the case of two particles localized in the sinusoidal field that is switched off for a small time interval.

A. Pulsed potential

Here, the two interacting particles run in opposite directions along a Si quantum wire. The external sinusoidal potential is switched on at t_{on} and for a time interval $\Delta\tau$. The Hamiltonian of the system reads

$$H(x_a, x_b) = H_{on-off}(x_a) + H_{on-off}(x_b) + \frac{e^2}{\epsilon\sqrt{(x_a - x_b)^2 + d^2}} \quad (5)$$

where H_{on-off} is the single-particle Hamiltonian given in Eq. (2), ϵ is the silicon dielectric constant and d represents the thickness of the wire, here and in the following sections fixed at 1 nm.

The two carriers have the same spin (up) and are obviously indistinguishable, so that the quantum state describing the system is given by

$$|\Psi\rangle = \frac{1}{\sqrt{2}} \left(|\psi\phi\rangle - |\phi\psi\rangle \right) |\uparrow\uparrow\rangle. \quad (6)$$

where both the wavefunctions corresponding to the states $|\psi\rangle$ and $|\phi\rangle$ are of the type defined in Eq. (1). The initial spread of the wavepackets and the distance between their centers are

such that the Coulomb energy of the system is negligible at initial time. In Eq. (6) the ket $|\uparrow\rangle$ indicates spin up state.

To obtain the system evolution we solve the time-dependent Schrödinger equation for the two-particle wavefunction of Eq. (6). Once the real-space wavefunction is found at a given time step, we compute the two-particle density matrix $\rho = |\Psi\rangle\langle\Psi|$ and from the latter, we calculate the one-particle reduced density matrix ρ_r by tracing on the degrees of freedom of one of the two electrons. ρ_r is then used to evaluate the entanglement. In fact, it is well known that for a two-fermion system a good correlation measure is given by the von Neumann entropy of ρ_r ^{26,31}:

$$\varepsilon = -\text{Tr}[\rho_r \ln \rho_r] = \sum_{i=1} |z_i|^2 \ln |z_i|^2, \quad (7)$$

where $|z_i|^2$ are the eigenvalues of the matrix ρ_r .

As in the previous section, we consider pulses 0.1 ps and 0.2 ps long. This implies that each of the two carriers can gain or lose $\hbar k_0$ in its momentum and the corresponding wavefunction splits into three peaks. In Fig. 2 and 3 we report the time evolution of the entanglement when $\Delta\tau = 0.1$ ps and 0.2 ps respectively, for different values of t_{on} , i.e. the time at which the pulse is switched on. Since the electron-electron interaction builds up quantum correlations in a limited time interval (roughly corresponding to the width of the entanglement peak when no pulse is present: the solid line in Fig. 2 and 3) it is clear that by choosing different t_{on} one means to consider cases with the potential pulse taking place before ($t_{on} = 0$), during ($t_{on} = 0.4$ and $t_{on} = 0.7$), and after ($t_{on} = 0.9$) the scattering.

At the initial time, the von Neumann entropy is equal to $\ln 2$. This value is related to unavoidable quantum correlations due to the exchange symmetry and it does not represent a manifestation of a genuine entanglement^{26,31}.

In absence of pulse, the entanglement increases while the two electrons are approaching each other, it has a maximum when the centers of the two wave packets are at the minimum distance, and finally drops again to the initial value once the electrons get far apart. In this case, due to the small thickness of the quantum wire, the effective Coulomb interaction between the electron is sufficient to cause a complete reflection of the two particles and the corresponding Gaussian wave packets are reconstructed with opposite momenta, as can be seen from the top of panel of Fig. 4.

When the two particles are subject to a pulsed sinusoidal potential, the entanglement dy-

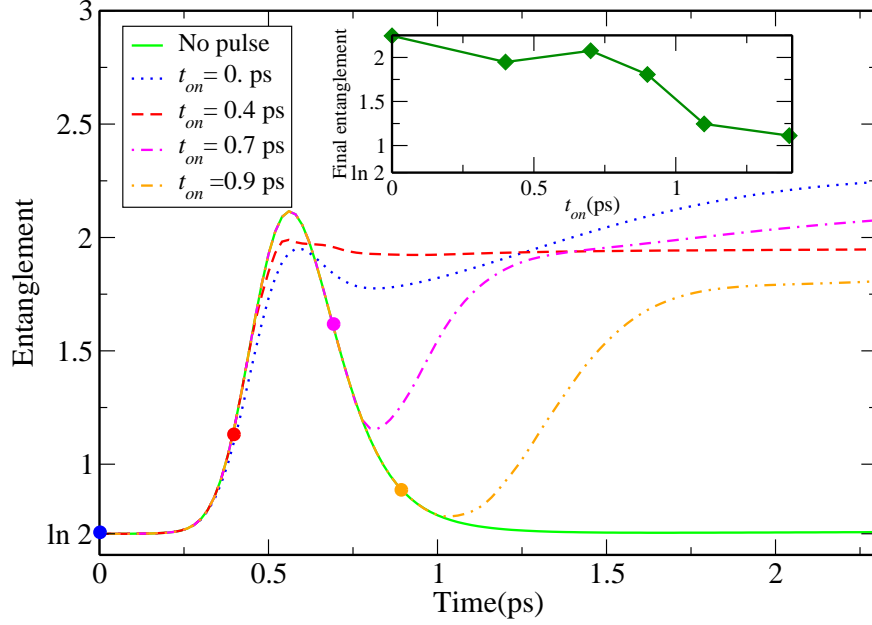


FIG. 2: Entanglement vs. time for different initial times of the pulse t_{on} . Here the pulse duration is $\Delta\tau = 0.2$ ps. At the initial time the two electrons have the same kinetic energy $E_k=10$ meV corresponding to $|k_{in}| = 0.290$ nm $^{-1}$ and are described by two wavepackets with mean dispersion $\sigma = 10$ nm moving in opposite directions. The filled circle on the curves indicate the four different t_{on} times. The inset shows the stationary values of the entanglement as a function of t_{on} .

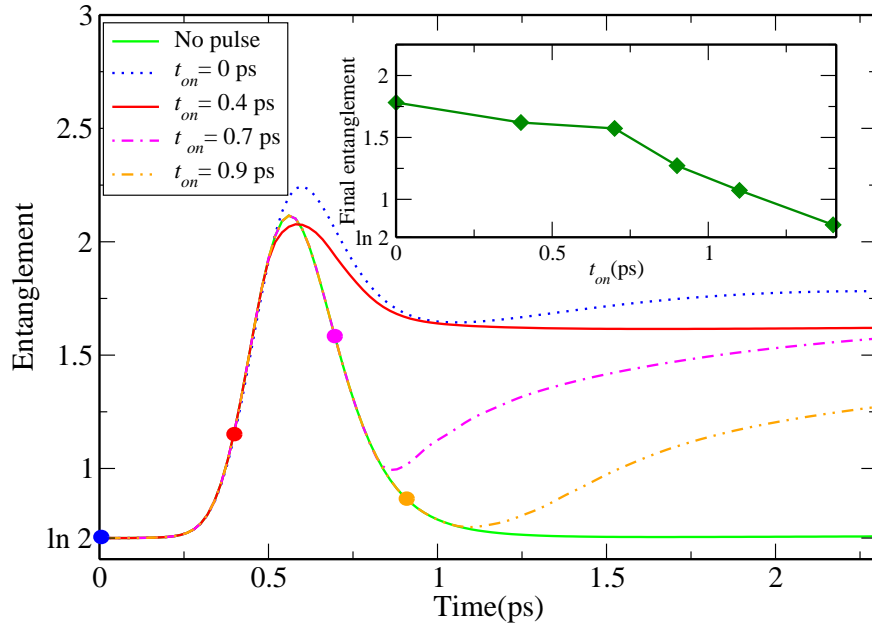


FIG. 3: Same as Fig. 2, with a pulse duration $\Delta\tau = 0.1$ ps.

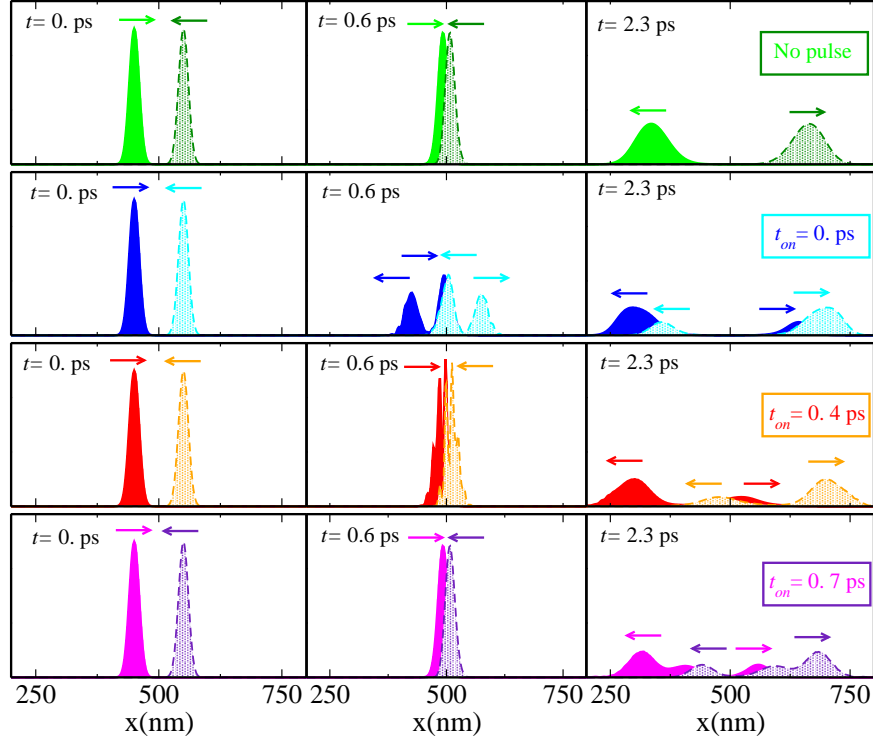


FIG. 4: Particle density at three different time steps, namely 0, 0.6 and 2.3 ps, for the case of no pulse (first row) and for different values of the initial time of the pulse t_{on} , as indicated. Here $\Delta\tau = 0.2$ ps. The solid shaded curve represents the probability density $\int |\langle x_a x_b | \psi \phi \rangle|^2 dx_a$ of the electron incoming from the right while the dashed curve describes the probability density of the electron incoming from the left.

namics depends strictly upon the details of the potential switching on and off. For example, for $\Delta\tau = 0.2$ ps and $t_{on} = 0$ ps, the peak of the entanglement is lower than the one found with no pulse. This is a consequence of the interaction with the sine-like potential that splits the wave function of each electron before the effect of the Coulomb potential becomes significant. Thus, the two reflected components will not take part into the scattering process and will not contribute to the entanglement formation (see Fig. 4). After the peak, for $t_{on} = 0.4$ ps the entanglement does not vary significantly with time, while in the case $t_{on} = 0$ it appears to increase. Such a difference can be ascribed to the fact that the splitting of the wavefunction can be or be not completed when the Coulomb interaction gets its maximum value.

For the last two cases of Fig. 2, $t_{on} = 0.7$ ps and $t_{on} = 0.9$ ps, the time evolution of the entanglement turns out to be quite peculiar. After the peak (due to the Coulomb

scattering) the entanglement exhibits the same decrease as in the case without the pulse, up to t_{on} , when the pulse is switched on. At the latter time, the wave function describing each electron is almost entirely reflected and splits in various peaks, as described above. Two of these, namely the components “reflected” by the pulse, propagate in opposite directions and approach each other. As a consequence, Coulomb interaction becomes effective again and gives rise to a second increase of the entanglement.

We report in Fig. 3 the results for $\Delta\tau = 0.1$ ps, showing a behavior similar to the previous case, with few, thus significative, differences. Specifically, for $t_{on} = 0$ ps we observe that the entanglement shows a peak higher than the one found in absence of the pulse. This behavior is different from the one found for $\Delta\tau = 0.2$ and can be ascribed to the diverse way of splitting of the electrons wavefunctions in the two cases, as described in Sec. II. Nevertheless we note that for $t_{on} = 0.7$ ps, after the peak (as high as the one found in absence of the external pulse) the entanglement decreases until t_{on} and then slowly increases, in qualitative agreement with what we obtained for $\Delta\tau = 0.2$ ps.

Some time after the Coulomb interaction and the pulse, the entanglement reaches a stationary value. This value is displayed in the insets of the Fig. 2 and 3 as a function of t_{on} . We observe that the largest final entanglement is always found when $t_{on} = 0$. In this case the wave functions split before the scattering and both the “accelerated” components of the electron and the central peaks, interact strongly during the Coulomb scattering.

Taking into account the results obtained in absence of pulse, we can therefore assume that the stationary values of the entanglement depend upon the transmission in the scattering event: they are greater for greater transmission probability of the particles. This is in qualitative agreement with the results of the theoretical investigations on the entanglement dynamics in scattering events in 1D structures^{5,7}.

B. Stationary potential

If the external sinusoidal potential is stationary, the electrons tend to localize in the minima. In this subsection, we study the evolution of the entanglement between two interacting electrons trapped in two adjacent minima. As in the previous case, we consider a Si quantum

wire as our prototype system. The two-particle Hamiltonian reads

$$H(x_a, x_b) = H_{stat}(x_a) + H_{stat}(x_b) + \frac{e^2}{\epsilon \sqrt{(x_a - x_b)^2 + d^2}}, \quad (8)$$

where

$$H_{stat}(x) = -\frac{\hbar^2}{2m} \frac{\partial^2}{\partial x^2} + \alpha \left(\sin\left(\frac{2\pi}{\lambda}x\right) + 1 \right) \quad (9)$$

is the single-particle Hamiltonian, with α representing the amplitude of the oscillation and λ the wavelength of the potential. The investigation of this model results to be of interest in the contest of electron transport in quantum wires assisted by SAWs²⁰. In fact, we can also assume that the Hamiltonian given in Eq. (8) describes a couple of electrons interacting with a travelling piezoelectric potential of the SAW, in the reference frame integral with the SAW itself.

It is worth noting that the use of SAW allows single-electron transport, in the sense that each electron moving in a 1D-channel can be trapped in a single minimum of the SAW. This prevents the spreading of the electron wave function and reduces undesired reflection effects, thus constituting a relevant improvement towards the implementation of a solid-state quantum gate based on coupled quantum wires^{9,20,21}.

In the analysis of charge transport assisted by SAWs, electrons are usually described by means of single-particle wave functions^{20,22,23,24,25}. This means that the quantum correlations between the particles due to their Coulomb interaction is neglected. Such an approximation is obviously the better the longer is the wavelength of the periodic potential. However, we aim at giving a quantitative estimation of the quantum correlation created in such a system, thus laying more solid foundations to the above approximation.

In our numerical calculation we have taken the amplitude of the oscillation α equal to 50 meV, corresponding to the value of the SAW amplitudes in the experimental setups²⁵. We consider two electrons with the same spin. The quantum state describing the system at the initial time is

$$|\Phi\rangle = \frac{1}{\sqrt{2}} \left(|\chi\varphi\rangle - |\varphi\chi\rangle \right) |\uparrow\uparrow\rangle. \quad (10)$$

The wavefunctions corresponding to the states $|\chi\rangle$ and $|\varphi\rangle$ are two eigenstates of the single-particle Hamiltonian of Eq. (9) describing electrons trapped in two nearest minima, as can be seen from the inset of the Fig. 5.

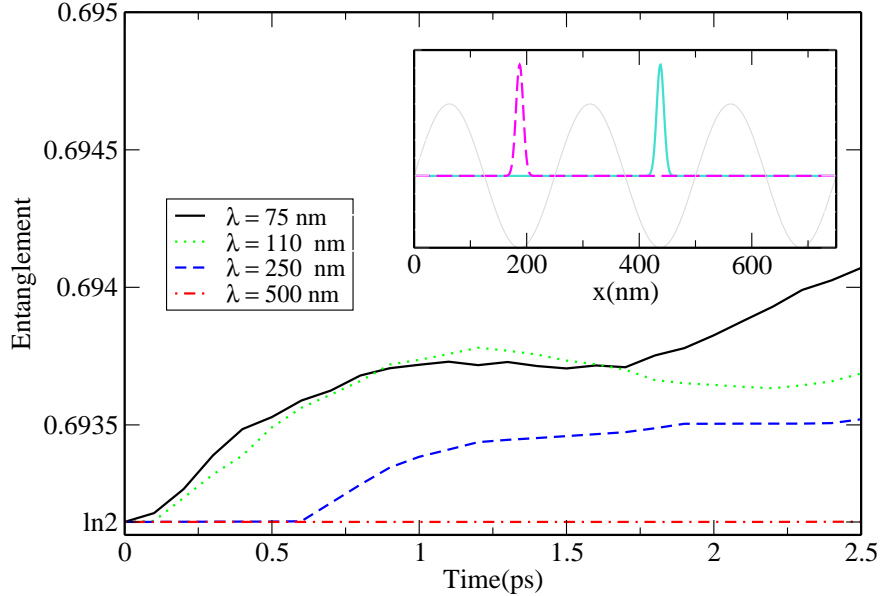


FIG. 5: Entanglement as a function of time for different values of the external potential wavelength λ : 75 nm (solid line), 110 nm (dotted line), 250 nm (dashed line), and 500 nm (dash-dotted line). The inset shows the square modulus of the initial two-particle wavefunction describing the electrons trapped in the two nearest minima of a sinusoidal potential (thin gray line). Note the scale on the vertical axis: the entanglement is almost constant in all the cases considered.

In the same figure, we report for different values of the wavelength λ of the sinusoidal potential, the time evolution of the entanglement, computed by using Eq. (7) through the von Neumann entropy of the one-particle reduced density matrix. At the initial time, no correlation is present, apart from the one due to the exchange symmetry. As time increases the entanglement does not vary significantly (only a few percentages of the initial value), though it is higher for smaller wavelengths, as expected. We stress that the abscissa scale of Fig. 5 is very expanded and that the wiggles in the curves have a numerical origin.

Since the entanglement between the electrons remains essentially constant, one can immediately conclude that during the time evolution of the two-particle wave function, the Coulomb interaction does not become sufficiently strong to build up significant quantum correlations between the two electrons. This implies that the time evolution of the system with SAWs can be studied in terms of the dynamics of two non-interacting single-particle wavepackets.

These results (obtained with physical parameters corresponding to the experimental se-

tups) suggest that the description of the single-electron transport assisted by SAWs in quantum wires in terms of single-particles wavefunctions represents a very good approximation for SAWs wavelength of the order of few hundreds of nanometres, as commonly used in the experimental apparatus^{22,23,24,25}.

C. Off-on switching potential

In this subsection we analyze the effect of the removal, for a short time interval, of the SAW potential described above. In particular, we are interested in the evolution of the entanglement between two electrons initially trapped in two nearest minima. The dynamics of the two particles is again 1D and the coupling originates from their mutual Coulomb interaction. The Hamiltonian of the system has the form

$$H(x_a, x_b) = H_{off-on}(x_a) + H_{off-on}(x_b) + \frac{e^2}{\epsilon\sqrt{(x_a - x_b)^2 + d^2}}, \quad (11)$$

where the single-particle Hamiltonian $H_{off-on}(x_a)$ is given by

$$H_{off-on}(x) = -\frac{\hbar^2}{2m} \frac{\partial^2}{\partial x^2} + \alpha [\theta(-t) + \theta(t - \Delta T)] \left(\sin\left(\frac{2\pi}{\lambda}x\right) + 1 \right). \quad (12)$$

Here we assume that, at the initial time $t = 0$, the external potential is abruptly switched off and then turned on again after a time interval ΔT .

Once again, we consider two electrons described at the initial time by a localized eigenstate of the sinusoidal potential of Eq. (12). Therefore, the two-electron system is again in the quantum state $|\Phi\rangle$ given in Eq. (10). As an example, we examine the case of a sinusoidal potential with a wavelength $\lambda = 110$ nm. In fact, we found that for longer wavelengths the switching off and on of the external potential does not lead to significant effects on the entanglement since the two particles remain at a distance at which the Coulomb interaction is rather weak.

In the top panel of Fig. 6 we report the time evolution of the entanglement for various ΔT , ranging from 0.3 to 0.6 ps. We observe that the entanglement increases with time and exhibits a sort of double step structure. Finally it reaches a stationary value that strictly depends upon ΔT . In other words, the electrons get more correlated for larger ΔT . To get a better insight into the process, we need to take into account the dynamics of the real-space two-particle wavefunction. Its initial peaks, describing the localized states of the two

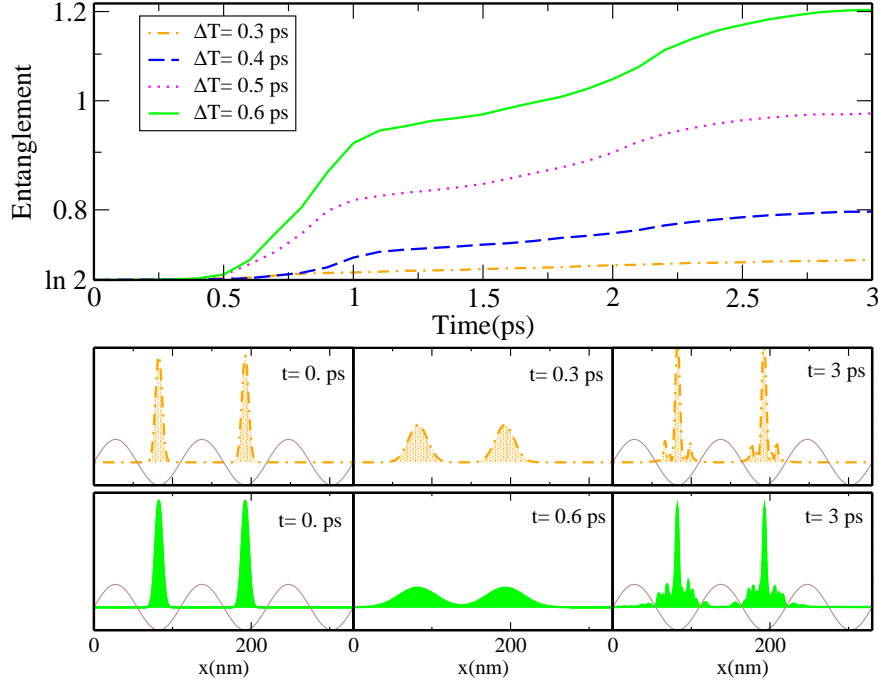


FIG. 6: Top panel: entanglement as a function of time for four different values of the time interval ΔT without the sinusoidal potential. The amplitude of the oscillation is 50 meV and the wavelength 110 nm in order to mimic a SAW potential. Bottom panel: square modulus of the two-particle spatial wavefunction $\langle x_a x_b | \chi \varphi \rangle$ evaluated at different time steps for two values of ΔT : 0.3 ps (dash-dotted line in the upper row of graphs) and 0.6 ps (solid-shaded curve in the lower row graphs). The thin solid line sketches the sinusoidal potential, when present.

electrons, spread as the external potential is removed. Therefore, for sufficiently long ΔT each peak can overlap with the other (see bottom panel of Fig. 6). This gives rise to a strong building up of quantum correlations, due to Coulomb interaction. Such an effect is obviously stronger when the sine-like potential is turned off for a longer time. After the potential is turned on again, i.e. for $t > \Delta T$, the wave packet is not smooth anymore, but it shows rapid oscillations. This affects the spatial overlap described above, which is responsible of the entanglement formation, thus leading to the peculiar double step structure observed in Fig. 6.

The results presented in this section can be also considered as an additional theoretical confirmation that the use of SAWs to drive electrons along quantum wires prevents the spreading of the spatial wavefunction and allows to suppress the effects of electron-electron correlation due to the Coulomb interaction. On the other hand, if the travelling periodic

potential is instantaneously turned off and then on, the electrons get quickly entangled.

IV. SUMMARY AND CONCLUSIONS

The growing interest in the entanglement phenomena in solid state systems^{3,4,9,10,11} led us to analyze the electron-electron entanglement dynamics in a rather peculiar model that has important applicative perspectives but whose simplicity makes it of general interest. In particular, the appearance of quantum correlations between two scattering carriers is a direct consequence of their mutual Coulomb repulsion during the scattering event, while the external periodic potential represents a mean to tailor the electron-electron interaction and to localize the particles. We stress that the equations of motion of the system under study are the same that describe the scattering of electrons by a standing laser wave^{16,17,18,19}, where the particles can change their momentum by an integer multiple of $\hbar k_0$, with k_0 the wave vector of the real-space modulation of the potential. Our single-particle time-dependent simulations show directly how the momentum gain or loss is affected by the switching-on time of the sinusoidal potential. In particular the use of pulses in the range of few tenths of picoseconds leads to a variation of a single $\hbar k_0$ quantum in the momentum of the particle.

The issues described above allowed us to explain the entanglement behavior in a two-electron scattering and our two-particle simulations gave a direct insight on the origin of the correlations. In fact, we showed that the non-separability of the two-particle state is mainly originated by the splitting of the spatial wave function brought about by the interaction with the potential pulse. As a matter of fact, our results show that the two particles get more correlated for longer pulses. Moreover, the time of the entanglement formation, i.e. the time at which the entanglement reaches its stationary value, is strictly related to the time of the initial switching-on of the sinusoidal potential. On the other hand, the final value of the entanglement depends upon the ratio between the transmitted and the reflected components of the wave function^{5,7}. We stress that the above finding shows that the final entanglement will be maximum for the specific system parameters (e.g. the wire dimension) that maximize the splitting of the wave function after the scattering.

In the following subsection, we addressed the entanglement created by the Coulomb interaction between two electrons localized into two nearest minima of a standing SAW potential of wavelength comparable or smaller than that of Refs. 22,23,24,25. We remark

here that our results confirm that the two particles remain essentially uncorrelated and that a single-particle modelling is suitable for those systems. This validates a number of theoretical investigations on the dynamics of single electrons trapped into SAW minima.

Finally, we have analyzed the effect of a brief switching off of the SAW potential: as for the free-particle scattering, the entanglement increases with time and reaches a stationary value that is “frozen” when the potential is restored. In particular, we find that the particles get more correlated for longer switching-off time intervals, due to the larger overlap between the spreading real-space wave functions. As a consequence, this system cannot be described in terms of single-particle states. On the contrary, it represents a suitable candidate for the controlled generation of bipartite entanglement.

References

- * Electronic address: buscemi.fabrizio@unimore.it
- ¹ A. Peres, *Quantum Theory: Concepts and Methods* (Kluwer Academy Publishers, The Netherlands, 1995.)
- ² D. Giulini et al., *Decoherence and the Appearance of a Classical World in Quantum theory* (Springer, Berlin, 1996.)
- ³ A Tal and G. Kurizki, Phys. Rev. Lett., **94**, 160503 (2005)
- ⁴ F. Buscemi, P. Bordone and A. Bertoni, Phys. Rev. B, **76**, 195317 (2007).
- ⁵ D. Gunlycke, J.H. Jefferson, T. Rejec, A. Ramsak, D.G. Pettifor and G.A.D. Briggs, J. Phys.: Condens. Matter **18**, S851-S866 (2006).
- ⁶ A. T. Costa, Jr. and S. Bose and Y. Omar, Phys. Rev. Lett. **96**, 230501 (2006).
- ⁷ A. Bertoni, J. Comp. Elec., **2**, 291 (2003).
- ⁸ L.D. Contreras-Pulido and F. Rojas, J. Phys.: Condens. Matter **18**, 9971 (2006).
- ⁹ A. Bertoni, P. Bordone, R. Brunetti, C. Jacoboni, and S. Reggiani, Phys. Rev. Lett., **84**, 5912 (2000).
- ¹⁰ W.D. Oliver, F. Yamaguchi, Y. Yamamoto, Phys. Rev. Lett. **88**, 037901 (R) (2002).
- ¹¹ A. Ramsak, J. Mravlje, R. Zitko, and J. Bonca, Phys. Rev. B **74**, 241305(R) (2006).

- ¹² T.P. Devereaux and R. Hackl, *Rev. Mod. Phys.*, **79**, 175 (2007).
- ¹³ S. Sepke, Y.Y. Lau, J.P. Holloway and D. Umstadter, *Phys. Rev. E*, **72**, 026501 (2005).
- ¹⁴ C.J Pethick and V. Thorsson, *Phys. Rev. D*, **56**, 7548 (1997).
- ¹⁵ P.L Kapitzza and P.A.M Dirac, *Proc. Phil. Soc.*, **29**, 297 (1933).
- ¹⁶ H Batelaan, *Rev. Mod. Phys.*, **79**, 929 (2007).
- ¹⁷ V.I Minogin, M.V. Feredov and V.S. Letokhov, *Opt. Commun.*,**140**, 250 (1997).
- ¹⁸ M.A Efremov, and M.V. Feredov , *J. Exper. Theor. Phys.*, **89**, 460 (1999).
- ¹⁹ M.A Efremov, and M.V. Feredov, *J. Phys.B*, **33**, 4535 (2000).
- ²⁰ C.H.W Barnes, J.M Shilton and A.M Robinson, *Phys. Rev. B*, **62**, 8410 (2000).
- ²¹ M. Rosini, A. Bertoni, P. Bordone, and C. Jacoboni, *J. Comp. Elec.*, **3**, 443 (2004) .
- ²² J.M Shilton, V.I. Talyanskii, M. Pepper, D.A. Ritchie, J.E.F. Frost, C.J.B. Ford, C.G. Smith and G.A.C. Jones, *J.Phys. Cond. Matter*, **8**, L531 (1996).
- ²³ V.I. Talyanskii, J.M Shilton, M. Pepper , C.G. Smith, C.J.B. Ford, E.H. Linfield, D.A. Ritchie, and G.A.C Jones, *Phys. Rev. B*, **56**, 15180 (1997).
- ²⁴ J. Cunningham, V.I. Talyanskii, J.M. Shilton, M. Pepper, M.Y. Simmons and D.A. Ritchie, *Phys. Rev. B*, **60**, 4850 (1999).
- ²⁵ J. Ebbeke, N.E. Fletcher, T.J.B.M. Jansenn, F.J. Ahlers , M. Pepper M, H.E. Beere and D.A. Ritchie, *Appl. Phys. Lett.*, **84**, 4319 (2004).
- ²⁶ F. Buscemi , P. Bordone, and A. Bertoni, *Phys. Rev.A*, **73** 052312 (2006).
- ²⁷ R. Brunetti , C. Jacoboni and F. Rossi, *Phys. Rev. B*, **39**, 10781 (1989).
- ²⁸ J. Mauritsson, P. Johnsson, E. Gustafsson, A. L’Huillier, K.J Schafer, and M.B. Gaarde, *Phys. Rev. Lett.*,**97**, 013001 (2006).
- ²⁹ M. Frasca, *Phys.Lett. A* **231** 344 (1997)
- ³⁰ S.A Gardiner and J.I. Cirac and P. Zoller, *Phys. Rev. Lett.*,**79**, 4790 (1997).
- ³¹ J. Schliemann, J.I. Cirac, M. Kus, M. Lewenstein and D. Loss, *Phys. Rev. A* **64**, 022303 (2001)